

## INFLUENCE OF SINTERING TEMPERATURE ON THE STRUCTURE OF YTTRIUM BASED PHOSPHOR NANOPARTICLES

Vasilica ȚUCUREANU<sup>1,2,\*</sup>, Alina MATEI<sup>1</sup>, Andrei AVRAM<sup>1</sup>,  
Marian Cătalın POPESCU<sup>1</sup>, Mihai DĂNILA<sup>1</sup>, Marioara AVRAM<sup>1</sup>,  
Cătalın Valentin MĂRCULESCU<sup>1</sup>, Bianca Cătălina ȚÎNCU<sup>1</sup>,  
Tiberiu BURINARU<sup>1</sup>, Daniel MUNTEANU<sup>2,\*</sup>

<sup>1</sup>National Institute for Research and Development in Microtechnologies, IMT-Bucharest,

<sup>2</sup>Transilvania University of Brasov, Department of Materials Science,

\*Corresponding authors: vasilica.tucureanu@imt.ro, danielmunteanu@unitbv.ro

### ABSTRACT

*Yttrium-based phosphor materials belonging to the class known as garnets have witnessed a strong return with the development of the first white LEDs. Among these materials, yttrium aluminum garnet doped with cerium has become the best known, being successfully used in generating white light, due to its capacity to convert the blue light emitted by a GaN chip. But its use in optoelectronic applications is subject to the achievement of parameters such as: purity of the crystal phase and particles size in the nanoscale range. In this study, we present a modified sol-gel method for the synthesis of yttrium aluminum garnet doped with cerium (YAG:Ce). In the end, heat treatment will be carried out at various temperatures and the effect of sintering temperature on the crystal phase and morphology will be studied. To highlight the phase transition from amorphous to crystalline state, a Rigaku SmartLab X-ray Diffraction System was used. Moreover, by the X-Ray diffraction pattern we evidenced the presence of the intermediate phases such as the main oxides, the metastable phases with perovskite (YAP) and monoclinic (YAM) structure and finally the garnet phase (YAG). The presence of the dopant in the crystalline structure was demonstrated. The microstructure and morphology evolution of the particles were assessed by using the FEI Nova NanoSEM system. Getting garnet phase and particles with spherical and smooth surfaces at the nanoscale range after a sintering treatment at 1100° C indicates a phosphor applicable in optoelectronics.*

KEYWORDS: phosphor, YAG:Ce, sol-gel process

### 1. Introduction

The international strategy in the field of lighting is aimed at finding new lighting sources with lower power consumption in order to minimize the electricity consumption. For this purpose, the RGB system has been used, a system based on the use of red-green-blue individual LEDs to generate white light. But disadvantages such as the varying degree of LED degradation, circuit complexity, high cost, etc, made this system non-usable for general lighting. However, this white light producing system remains used in the field of video panels [1-3]. Another white light generation system using LED chips, which has proven its viability since 1996, is based on the use of one or more phosphors along with a blue / UV

structure. It is expected that these devices based on LEDs will lead to the replacement of classical lighting systems due to advantages such as: low energy consumption, high power efficiency, long life time, high shock resistant, small size, and so on. But in this case, there are problems because the quality of light emitted in a white LED is strongly influenced by the structure and morphology of the luminous material [4, 5].

A phosphor is a material that emits photons at a wavelength greater than the excitement source. Yttrium based phosphor, known as cerium-doped yttrium aluminum garnet (YAG:Ce), is a synthetic crystalline material from garnet family and the most widely used as luminescent material to generate white light in an LED [6, 7]. The only existing method for

obtaining YAG:Ce at an industrial level is the solid-state method between the main oxides at high temperature (1600-1900 °C) and high production cost. High temperature is necessary for crystallization but the phosphors resulting under these conditions have a low production yield due to the large variation in grain size and the presence of secondary phases that act as impurity with consequences on phosphors quality [8, 9]. In order to obtain phosphors with superior optical qualities at a low-cost price, wet methods (method as: sol-gel, coprecipitation, solvo / hydrothermal, spray-pyrolysis etc.), have gained ground. Despite the existence of a very large number of alternative bottom-up methods, obtaining a single phase in garnet form (with a  $Y_{3-x}Ce_xAl_5O_{12}$  (YAG) molecular formula) is not a simple task [10-19]. In the crystalline system can coexist the basic oxides ( $Al_2O_3$ ,  $Y_2O_3$ ), yttrium aluminum monoclinic (YAM,  $Y_4Al_2O_9$ ), yttrium aluminum perovskite (YAP,  $YAlO_3$ ) and yttrium aluminum garnet (YAG,  $Y_3Al_5O_{12}$ ) [19-21]. Moreover, the presence of cerium ions as secondary cerium oxide ( $CeO_2$ ,  $Ce_2O_3$ ) phases in the garnet network leads to the strong degradation of phosphor quality.

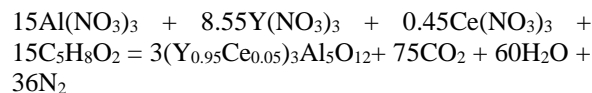
The main objective of this investigation was the fabrication of a YAG:Ce by a modified sol-gel method under the presence of DMSO and CTAB for a better control in order to obtain single garnet phase of phosphor at nanometrical scale. The structural and morphological evolution of the phosphor powder has been studied according to the sintering temperature.

## 2. Experimental procedure for the synthesis and characterization of yttrium based phosphor

In the present paper we proposed a modified sol-gel method for yttrium based phosphor synthesis. The following raw materials were used to synthesize the YAG:Ce phosphor: yttrium oxide ( $Y_2O_3$ ), aluminum oxide ( $Al_2O_3$ ), dimethyl sulfoxide (DMSO,  $(CH_3)_2SO$ ), acetylacetone (AcAc,  $CH_3COCH_2COCH_3$ ), cetrimonium bromide (CTAB,  $(C_{16}H_{33})N(CH_3)_3Br$ ), nitric acid ( $HNO_3$ ) (from Sigma Aldrich, all analytical grade). Cerium oxide ( $CeO_2$ ) at nanoscale was synthesized by coprecipitation method in our labs [22].

The oxides were dissolved in the nitric acid. The solution was stirred continuously and kept at 80° C. While maintaining the system under reflux conditions, AcAc, DMSO and CTAB were added. In the process, we considered the reaction below as ideal, and we used the raw material in stoichiometric report for the preparation of the YAG doped with 5% cerium ion. The chelating agent was added in excess,

in a molar ratio 3 times greater than the theoretical reaction.



Reaction conditions were maintained for 6 hours, after which the reflux was removed and allowed to stand for several days for bulk polymerization. The quality of the phosphate based on yttrium is strongly influenced by the thermal treatment stage. In our work the annealing has being carried out in two steps. The pre-sintering or slow evaporation was the stage controlled by DMSO and CTAB, used to provide better control over nanoparticle morphology. The utility of DMSO can be explained by the higher boiling temperature of the water which allows a slower evaporation of the liquids from the network., The CTAB also has anchoring capacity or selectivity to various crystal facets. Particular attention has been paid to pre-sintering up to 400 °C when the nitrates and all organic compounds decomposition occur. Temperature was incremented with 4 °C/min and maintained at 400 °C for 24 hours, resulting in the formation of a brown phosphor precursor. The appearance of YAG:Ce yellow phosphors was observed after treatment in air at 1100 °C for 48 hours (4 samples were taken after heat treatment in the range of 900-1100 °C).

To observe the influence of the sintering temperature on the YAG:Ce phosphors structure, Rigaku SmartLab X-ray Diffraction System was used with  $CuK\alpha$  radiation in the  $2\theta$  range from 20° to 70°. Scherrer's equation was used to calculate the average crystallite size. The dopant presence in the crystalline network was confirmed using energy dispersive X-ray spectroscopy (EDX) for the phosphors elemental composition analysis. EDX spectra were collected with a TESCAN having an EDAX facility, operated at 10 kV. Moreover, using Fourier Transform Infrared (FTIR) spectrometry (Bruker Optics, Tensor 27) and KBr disk technique, we have highlighted the existence of the Ce-O bond in the crystalline network. The spectra were taken in the wavenumber 4000-400  $cm^{-1}$  by averaging 64 scans and with a resolution of 4  $cm^{-1}$ . The microstructure and morphology evolution of the particles were determined using field emission scanning electron microscopy (FE-SEM). The SEM images for the powder samples were taken with an FEI Nova NanoSEM 630 system. In order to increase the image quality, before the SEM examination, the yellow phosphors were dispersed into ethanol, ultrasonicated for 30 min., dip-cast onto the surface of silicon wafers and coated with a thin gold layer.

### 3. Results and discussions

The quality of phosphors based on yttrium is determined by its structure and morphology, the purity of the garnet phase, the shape and size of the particles. The XRD diagrams were used in order to study the crystal structures of the phosphor, purity, crystallite size and strain.

The YAG crystal structure has a 160-atom body-centered cubic (bcc) unit cell and Ia-3d (230) space group. From a theoretical point of view, the evolution of a sample of phosphors after the thermal treatment is from raw material ( $Al_2O_3 - Y_2O_3$ ) to amorphous, YAP, YAM, hexagonal and / or orthorhombic YAP and YAG phase [21]. However, in practice, in the luminescent material several phases coexist, which was seen in the XRD diagrams. All single lines can be indexed (Table 1) for the samples and are attributed to garnet crystal structure and to the intermediate phase caused by incomplete processes [20].

Figure 1 shows X-ray diffraction pattern of the phosphor precursor and for the material after annealing at temperatures of 900-1100 °C.

In the XRD graph of the phosphor precursor (fig 1 [1]) may be observed an amorphous compound. For the phosphor annealed at temperature over 900 °C (fig 1 [2]) the transition from amorphous to crystalline phases, and the existence of the YAP as the predominant phase were observed. The samples annealed at 900-1050 °C (Fig. 1 [3], 1 [4], 1 [5]) revealed the YAG as the predominant phase and the presence of reaction intermediate. XRD analysis (Fig. 1 [6]) for the sample undergoing a heat treatment at 1100 °C shows that this temperature is sufficient to obtain a single phase of garnet. All lines were identified and indexed to the YAG phases, thus confirming the transformation of all intermediates

into the garnet structure. The samples sintered over 950 °C, indicate a peak centered at about  $2\theta = 33.4^\circ$  which corresponds to the crystalline plane with Miller indices of (420) from YAG structure, suggesting that the predominant phase is the garnet. In the case of the sample annealed at 900 °C we noticed that the main peak is at  $2\theta = 34.29^\circ$ , indicating that the main phase is YAP phase. Using the main peak and the Scherrer equation, the average crystallite size was calculated. Figure 2 shows the crystallite size variation as a sintering temperature function, noticing a decrease in the average crystallite size to a certain temperature (1100 °C). The average crystallite size calculated for the YAG:Ce is 36 nm. The possibility of increasing the average size of the crystals appears at high temperature and sintering time.

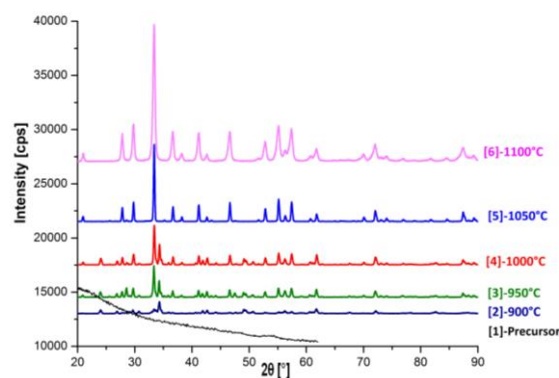


**Fig. 1.** X-Ray diffraction pattern of YAG:Ce phosphor samples annealed at different temperature: (1)-precursor, (2) sintering at 900 °C, (3) sintering at 950 °C, (4) sintering at 1000 °C, (5) sintering at 1050 °C and (6) sintering at 1100 °C

**Table 1.** Crystalline planes for yttrium based phosphor after annealing at 900-1100 °C

Crystalline phase	$2\theta_B$ [°] 1100 °C	$2\theta_B$ [°] 1050 °C	$2\theta_B$ [°] 1000 °C	$2\theta_B$ [°] 950 °C	$2\theta_B$ [°] 900 °C
YAG	20.98, 27.83, 29.72, <b>33.39</b> , 36.60, 38.18, 41.21, 42.62, 46.66, 51.66, 52.78, 55.12, 56.28, 57.39, 60.75, 61.75, 70.04, 72.03, 74.03, 76.96, 81.79, 84.64, 87.38, 89.30.	20.96, 27.81, 29.78, <b>33.40</b> , 36.70, 38.25, 41.20, 42.61, 46.65, 51.63, 52.85, 55.11, 56.34, 57.42, 60.72, 61.81, 70.05, 72.07, 74.05, 76.93, 81.73, 84.61, 87.46, 89.31.	20.98, 27.81, 29.78, <b>33.40</b> , 36.70, 38.24, 41.22, 42.69, 46.67, 51.66, 52.83, 55.16, 56.25, 57.46, 60.75, 61.82, 70.07, 72.04, 74.04, 76.94, 81.73, 84.55, 87.40, 89.26.	20.90, 27.71, 29.72, <b>33.43</b> , 36.60, 38.22, 41.23, 42.59, 46.59, 51.59, 52.77, 55.12, 56.19, 57.46, 60.64, 61.74, 70.01, 72.07, 74.02, 76.81, 81.73, 84.54, 87.38, 89.25.	20.95, 27.83, 29.68, 33.60, 36.57, 38.16, 41.16, 42.72, 46.65, 52.78, 55.11, 56.20, 57.44, 60.58, 61.71, 72.13, 76.90, 87.34, 89.17.
YAP	-	35.18.	24.08, 26.94, 34.30, 34.70, 35.89, 41.86, 49.46, 61.17, 67.58.	23.99, 26.88, 34.18, 34.60, 35.18, 35.85, 41.82, 49.41, 61.09, 67.54.	24.01, 26.96, <b>34.29</b> , 34.55, 35.87, 41.87, 49.36, 61.05, 67.56.
YAM	-	-	-	29.13.	29.10.
$Al_2O_3$	-	-	25.63, 30.81, 40.70, 43.44, 44.20.	25.57, 30.73, 40.65, 43.34, 44.13.	25.52, 30.70, 40.65, 43.45, 44.25.
$Ce_2O_3$	-	28.58, 47.51.	28.64, 47.69.	28.57, 47.54.	28.68, 47.68.

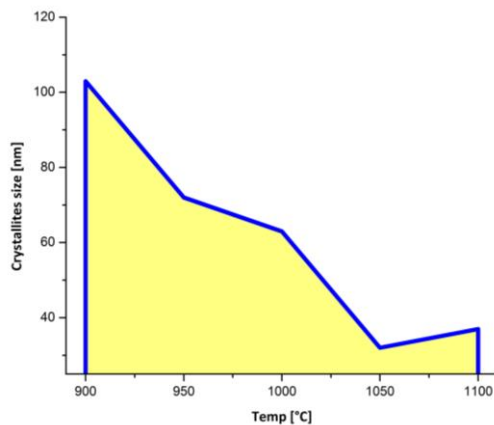


**Fig. 2.** Variation of crystallite average size of the YAG:Ce samples as a function of sintering temperature

Figure 3 presents the strain of the network as a function of the temperature, showing a direct proportional decrease with the temperature increase, which is explained by the decrease of the stress in the network as a result of the removal of the secondary phases from the final product.

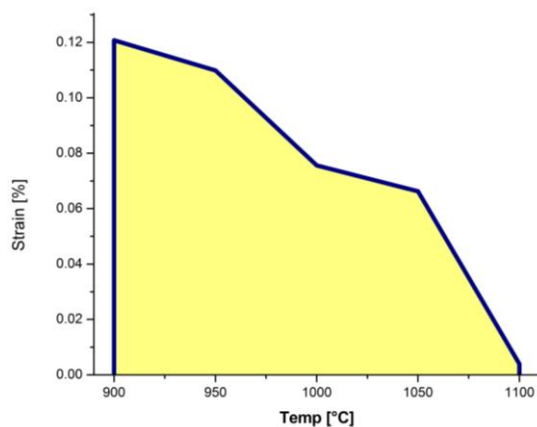


**Fig. 3.** Strain variation of the YAG:Ce crystalline samples as a function of sintering temperature

Further annealing of the powder over 1000 °C shows an increase of diffraction peak intensity due to the improved purity and crystallinity. The largest and sharpest peaks can be observed for phosphor powder treated at 1100 °C. The presence of cerium ions is only observed in the annealed samples up to 1050 °C, due to the incomplete transformation process. For the sintered sample at 1100 °C, the complete substitution of  $Y^{3+}$  with  $Ce^{3+}$  does not disturb the crystalline structure of the samples, appearing only a small change in the lattice parameters due to the difference

in the ionic radii. The lattice parameters of the YAG:Ce were found to be 12.0028 Å.

In terms of qualitative analysis, in the energy-dispersive X-ray spectrum in Figure 4 we can see peaks that correspond to the atoms of O (O(K) at 0.53 keV), Al (Al(K) at 1.49 keV), Y (Y(L) at 1.92 keV) and Ce dopant (Ce(L) at 4.8 keV). The quantitative analysis was based on the use of atomic percentages, from EDX data, for calculating the molecular formula of the yttrium based phosphor sample. The final composition was calculated and corresponds to theoretical  $Y_{2.81}Ce_{0.13}Al_{5.02}O_{12.04}$  formula, which suggests a good crystallinity and is very close to that of the target materials.

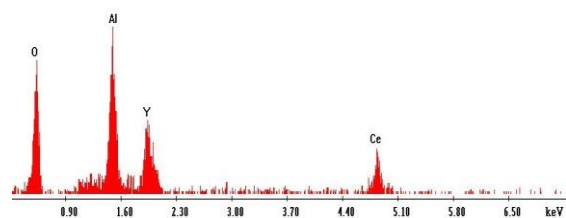


**Fig. 4.** EDX spectrum of a representative YAG:Ce phosphor powder

Moreover, the FTIR spectra (Fig. 5) for a YAG:Ce sample annealed at 1100 °C confirms the existence of Ce-O bond in the crystalline network.

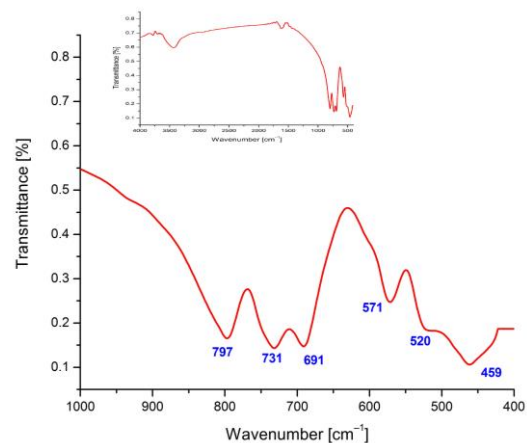


**Fig. 5.** FTIR spectrum for YAG:Ce phosphor powder

It is observed that the spectrum consists of significant absorption bands at the lowest frequencies (below 800  $cm^{-1}$ ), that has been assigned to the vibrations mode of the M-O bonds from the garnet structure. The bands centered at 797 and 691  $cm^{-1}$  occur from the stretching vibrations of the Al-O; the peak from 732  $cm^{-1}$  is assigned to Y-O, while the peak from 571  $cm^{-1}$  is assigned to Y-O-Al bonds. The

presence of the dopant in the sample was observed in the bands centered at 520 and 459  $\text{cm}^{-1}$  which can be attributed to the vibration mode of the Ce-O bonds from the garnet crystalline network [20]. The bands attributed to O-H bonds (3440 and 1636  $\text{cm}^{-1}$ ) are due to water absorption. No organic residue was observed in the spectrum.

Obtaining particles with spherical surface and at nanoscale is necessary to avoid scattering phenomena and to improve optical properties. Figure 6 shows SEM micrographs for precursor samples and treated

at temperatures between 900 and 1100 °C. The SEM micrograph for the precursor sample (Fig. 6 [1]) confirms the XRD observations of amorphous compound formation. The samples treated at temperatures up to 1050 °C (Fig. 6 [2]-6 [5]) present irregular particles with a heterogeneous distribution, thus confirming that the process is incomplete. The sintered sample at 1100 °C (Fig. 6 [6]), exhibits particles with spherical shape and smooth surface. An average particle size of about 40-60 nm was determined.

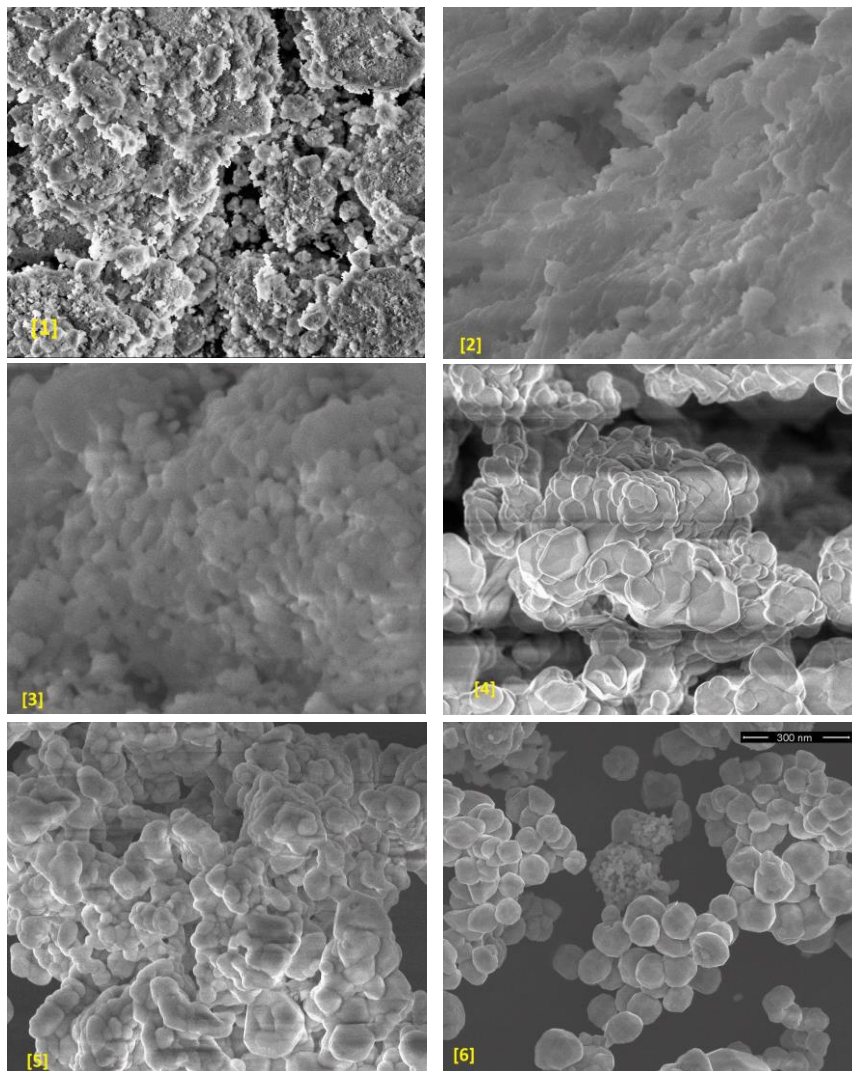


**Fig. 6.** SEM micrograph of the YAG:Ce phosphor samples sintered at different temperature: (1)-precursor, (2) sintering at 900 °C, (3) sintering at 950 °C, (4) sintering at 1000 °C, (5) sintering at 1050 °C, (6) sintering at 1100 °C

#### 4. Conclusion

Using a modified sol-gel method we synthesized a yellow garnet phosphor. The oxides and the acetylacetonate were used in the process as raw

materials and as chelating agent, respectively. CTAB and DMSO were used for morphology control. The thermal treatment was studied from the structural and morphological point of view. An amorphous precursor (at 900 °C) and transition to crystalline

phases (by annealing over 900 °C) was confirmed by the XRD diagrams. In the sample sintered at high temperature, the formation of YAG phases was observed. Only for phosphor annealed at 1100 °C YAG is the single-phase present. For the samples sintered at 900-1050 °C, the coexistence of Al<sub>2</sub>O<sub>3</sub>, Ce<sub>2</sub>O<sub>3</sub>, YAM, YAP, and YAG phases was determined. The existence of intermediate phases due to the incomplete process was also observed in the variance of the network strain. We noticed that the average particle size increases with increasing temperature for the samples sintered at 900-1100 °C. Using the EDX analysis, the main atoms were identified and the Y<sub>2,81</sub>Ce<sub>0,13</sub>Al<sub>5,02</sub>O<sub>12,04</sub> molecular formula was established. The presence of the dopant in the crystalline structure was evidenced by EDX and FTIR analyses. Peaks were observed in the FTIR spectrum, which can be assigned to the vibration mode of the M-O bonds from the garnet molecule. SEM micrographs come to confirm the XRD observation. The amorphous form of the precursor was observed, with irregular particles variation and heterogeneous distribution for the sample treated at 900-1050 °C and nanoparticles with spherical shape and smooth surface for the samples after treatment at 1100 °C.

### Acknowledgments

This work was supported by UEFISCDI in the Partnership Framework: PN-III-P2-2.1-PTE-2016-0145 (Project No. 46PTE/2016), PN-III-P2-2.1-PED-2016-0123 (Project No. 119/2017), PN-II-PT-PCCA-2013-4-0366 (Project No. 208/2014) and by National Basic Funding Program TEHNOSPEC - Project No. PN1632/2016.

This work was supported by a grant of the Ministry of National Education and Scientific Research, RDI Program for Space Technology and Advanced Research-STAR, project number 639/2017.

This paper is part of the Vasilica (Șchiopu) Țucureanu's PhD thesis, at Transilvania University of Brașov, Department of Materials Science, coordinated by Prof. dr. eng. Daniel Munteanu, to whom I am grateful for all the support and guidance.

### References

- [1]. Kim T., Lee J., *Template-free Synthesis and Characterization of Template-Free Synth. YAG:Ce NanoPhosphor* Bull. Korean Chem. Soc., 35, p. 2917-2921, 2014.
- [2]. Panatarani C., Joni I. M., *Challenging and development of phosphors for lighting applications*, AIP Conf. Proc., 1712, 020003(1-5), 2016.
- [3]. Pust P., Schmidt P. J., Schnick W., *A revolution in lighting*, Nat. Mater., 14, p. 454-458, 2015.
- [4]. Zhang L., Lu Z., Zhu J., Yang H., Han P., Chen Y., Zhang Q., *Citrate sol-gel combustion preparation and photoluminescence properties of YAG:Ce phosphors*, J. Rare Earths., 30, p. 289-296, 2012.
- [5]. Ryu H. Y., *Analysis on the luminous efficiency of phosphor-conversion white light-emitting diode*, J. Opt. Soc. Korea., 17, p. 22-26, 2013.
- [6]. Jang M. S., Choi Y. H., Wu S., Lim T. G., Yoo J. S., *Material properties of the Ce<sup>3+</sup>-doped garnet phosphor for a white LED application*, J. Inf. Disp., 17, p. 117-123., 2016.
- [7]. Haaheim J., DenBaars S., *A History of Solid State White Lighting the Evolution of GaN Nanowires, and New Potentials for White Light Generation Using InGaN Nanowires*, Dep. Electr. Comput. Eng. Univ. Calif. – St. Barbar, p. 1-15, 2002.
- [8]. Lee H. M., Cheng C. C., Huang C. Y., *The synthesis and optical property of solid-state-prepared YAG:Ce phosphor by a spray-drying method*, Mater. Res. Bull., 44, p. 1081-1085, 2009.
- [9]. Chou C. S., Wu C. Y., Yeh C. H., Yang R. Y., Chen J. H., *The optimum conditions for solid-state-prepared (Y<sub>3-x</sub>Ce<sub>x</sub>)Al<sub>5</sub>O<sub>12</sub> phosphor using the Taguchi method*, Adv. Powder Technol., 23, p. 97-103, 2012.
- [10]. Zhang X., Jin C., Zhang Y., Jia N., He W., *Synthesis of spherical yttrium aluminum garnet via a mixed solvothermal method*, RSC Adv., 4, p. 57452-57457, 2014.
- [11]. Yixuan R., Li G., Junguo R., *Effect of PEG Addition on the Properties of YAG:Ce Phosphor Synthesized via a Homogeneous Precipitation Method*, Rare Met. Mater. Eng., 44, p. 2100-2104, 2015.
- [12]. Wang B., Qi H., Han H., Song Z., Chen J., Shao J., *Structural, luminescent properties and chemical state analysis of YAG:Ce nanoparticle-based films*, Opt. Mater. Express, 6, p. 155-165, 2016.
- [13]. Tucureanu V., Matei A., Mihalache I., Danila M., Popescu M., Bita B., *Synthesis and characterization of YAG:Ce,Gd and YAG:Ce,Gd/PMMA nanocomposites for optoelectronic applications*, J. Mater. Sci., 50, p. 1883-1890, 2015.
- [14]. Trifonov Y. G., Kuznetsova D. E., Dosovitskii G. A., Omarov A. Y., Novoselov R. A., Tarasovskii V.P., *Preparation of Aluminum-Yttrium Garnet Luminescent Ceramic Alloyed with Cerium*, Refract. Ind. Ceram., 56, p. 271-275, 2015.
- [15]. Palmero P., Traverso R., *Co-precipitation of YAG powders for transparent materials: Effect of the synthesis parameters on processing and microstructure*, Materials (Basel), 7, p. 7145-7156, 2014.
- [16]. Ma R., Lu B., Cao H., Hu J., Zhang X., Qiu Q., Zheng R., Luo Z., Xue B., *Preparation and characterization of YAG:Ce thin phosphor films by pulsed laser deposition*, Int. J. Appl. Ceram. Technol, p. 1-9, 2017.
- [17]. Kaithwas N., Dave M., Kar S., Bartwal K. S., *Structural features of Ce doped YAG nanoparticles synthesized by modified sol-gel method*, Phys. E., 44, p. 1486-1489, 2012.
- [18]. He X., Liu X., Li R., Yang B., Yu K., Zeng M., Yu R., *Effects of local structure of Ce<sup>3+</sup> ions on luminescent properties of Y<sub>3</sub>Al<sub>5</sub>O<sub>12</sub>:Ce nanoparticles*, Sci. Rep., 6, p. 1-11, 2016.
- [19]. Chung D. N., Dinh N. N., Hieu D. N., Duong P. H., *Synthesis of cerium-doped yttrium aluminum garnet nanopowder low-temperature reaction combustion method*, VNU J. Sci. Math, 28, p. 53-60, 2012.
- [20]. Tucureanu V., Matei A., Avram A., *Synthesis and characterization of YAG:Ce phosphors for white LEDs*, Opto-Electronics Rev., 23, p. 239-251, 2015.
- [21]. Hess N. J., Maupin G. D., Chick L. A., Sunberg D. S., McCreedy D. E., Armstrong T. R., *Synthesis and crystallization of yttrium-aluminium garnet and related compounds*, J. Mater. Sci., 29, p. 1873-1878, 1994.
- [22]. Matei A., Tucureanu V. Tincu B., Popescu M., Romanita C., Cernica I., Dumitrescu L. G., *Experimental aspects for CeO<sub>2</sub> nanoparticles synthesis and characterization*, Sci. Conf. Dr. Sch., SCDS-UDJG 2017, p. 123-123, 2017.